Sclerostin Antibody Increases Bone Volume and Enhances Implant Fixation in a Rat Model

Amarjit S. Virdi, PhD, Min Liu, PhD, Kotaro Sena, DDS, PhD, James Maletich, BS, Margaret McNulty, PhD, Hua Zhu Ke, MD, and Dale R. Sumner, PhD

Investigation performed at the Department of Anatomy and Cell Biology, Rush University Medical Center, Chicago, Illinois

Background: Previous studies have demonstrated that sclerostin blockade is anabolic for bone. This study examined whether systemic administration of sclerostin antibody would increase implant fixation and peri-implant bone volume in a rat model.

Methods: Titanium cylinders were placed in the femoral medullary canal of ninety male Sprague-Dawley rats. One-half of the rats (n = 45) received murine sclerostin antibody (Scl-Ab, 25 mg/kg, twice weekly) and the other one-half (n = 45) received saline solution. Equal numbers of rats from both groups were sacrificed at two, four, or eight weeks after the implant surgery and the femora were examined by microcomputed tomography, mechanical pull-out testing, and histology.

Results: Fixation strength in the two groups was similar at two weeks but was 1.9-fold greater at four weeks ($p = 0.024$) and 2.2-fold greater at eight weeks ($p < 0.001$) in the rats treated with sclerostin antibody. At two weeks, antibody treatment led to increased cortical area, with later increases in cortical thickness and total cross-sectional area. Significant differences in peri-implant trabecular bone were not evident until eight weeks but included increased bone volume per total volume, bone structure that was more plate-like, and increased trabecular thickness and number. Changes in bone architecture in the intact contralateral femur tended to precede the peri-implant changes. The peri-implant bone properties accounted for 61% of the variance in implant fixation strength, 32% of the variance in stiffness, and 63% of the variance in energy to failure. The implant fixation strength at four weeks was approximately equivalent to the strength in the control group at eight weeks.

Conclusions: Sclerostin antibody treatment accelerated and enhanced mechanical fixation of medullary implants in a rat model by increasing both cortical and trabecular bone volume.

Clinical Relevance: Sclerostin antibody treatment may be useful for improving implant fixation.

Total joint replacement is a common and successful orthopaedic procedure that has successfully improved quality of life, especially for older individuals with osteoarthritis. However, poor implant fixation due to a variety of reasons including aseptic loosening remains a substantial problem, often necessitating revision total joint replacement[1]. The number of total joint replacement revision procedures performed annually in the U.S. is well over 70,000 and is expected to increase to more than 350,000 by 2030[1-3]. This prediction is worrisome because of the relatively high failure rate of revision total joint replacement[4,5]. One approach to reducing the risk of implant loosening is to enhance the amount of new bone formed around the implant in order to improve early stability of the implant[6,7] and possibly lessen the likelihood of later ingress of particulate debris at the interface and eventual loss of fixation through particulate-induced osteolysis[8]. Strategies for enhancing implant fixation include use of locally or systemically delivered growth factors such as bone morphogenetic protein (BMP) or transforming growth factor-beta[9-13] and pharmaceutical agents such as systemically delivered parathyroid hormone[14].

Sclerostin, a specific product of the SOST gene, is secreted by osteocytes and functions to limit bone formation[15-18]. Subjects with mutations in the SOST gene have high bone density[19]. Targeted deletion of the SOST gene in mice leads to

Disclosure: One or more of the authors received payments or services, either directly or indirectly (i.e., via his or her institution), from a third party in support of an aspect of this work. In addition, one or more of the authors, or his or her institution, has had a financial relationship, in the thirty-six months prior to submission of this work, with an entity in the biomedical arena that could be perceived to influence or have the potential to influence what is written in this work. No author has had any other relationships, or has engaged in any other activities, that could be perceived to influence or have the potential to influence what is written in this work. The complete **Disclosures of Potential Conflicts of Interest** submitted by authors are always provided with the online version of the article.

increased bone formation and bone strength[20,21]. Sclerostin is thought to negatively regulate bone formation by binding to cell surface receptors LRP5/6 and inhibiting Wnt/beta-catenin signaling[22-24] and/or inhibiting BMP activity[15,16]. Removing this inhibition, for instance by using a neutralizing antibody to sclerostin, leads to increased bone formation as demonstrated in the reversal of ovariectomy-induced low bone mass and strength in rats[25] and in osteoporotic patients[26]. Although BMP gene expression has been known to be upregulated during skeletal repair[27-34], more recently it has been shown that many genes in the Wnt signaling pathway are also upregulated[35-37] and that sclerostin antibody enhances fracture-healing in rodent and nonhuman primates[38]. These data support the rationale that sclerostin antibody treatment could improve the interfacial attachment between bone and implant, and ultimately improve the mechanical fixation of the implant. Indeed, fixation of screws placed in metaphyseal cortical bone increased following systemic administration of sclerostin antibody[39].

The rat marrow ablation model is being used by our group[40-43] and others[44-46] to examine fixation of implants. In the present study, we used this model system to determine whether blockade of sclerostin with a neutralizing antibody could enhance intramembranous bone formation and improve implant fixation. We hypothesized that the reduction in sclerostin activity by the antibody would boost osteogenesis around the implant and result in greater implant fixation strength.

Materials and Methods

Research Design

In a protocol approved by our Institutional Animal Care and Use Committee, a total of ninety 400-g (six-month-old) male Sprague-Dawley rats (Harlan Laboratories, Indianapolis, Indiana) were randomized to a control group (n = 45) and a sclerostin antibody treatment group (n = 45). Fifteen animals in each group were sacrificed at two weeks, four weeks, or eight weeks after unilateral placement of a titanium implant in the medullary canal of the left femur. The primary end points included assessment of peri-implant trabecular and cortical bone by microcomputed tomography (micro-CT) (n = 15 per group per time point), mechanical testing (n = 12 per group per time point), and qualitative histology (n = 3 per group per time point). We also examined trabecular and cortical bone from the contralateral femur (n = 15 per group per time point). The most important end point was fixation strength and, based on the initial sample size of twelve and allowing for attrition due to unexpected deaths or technical difficulties, we predicted that the power of the experiment would be 0.856 for a final sample size of ten per group and a standard deviation equal to 70% of the expected difference between the means of the groups[47]. Body weight was determined at the time of surgery and when the animals were killed. Descriptions of the implants, surgery, micro-CT scanning, mechanical testing, and histology are presented briefly here and in detail in the Appendix.

Implants

Dual acid-etched implants[48] (1.5 mm in diameter and 20 mm long) made from commercially pure titanium rods were used.

Surgery

An adaptation of the marrow ablation model[49] was used; the medullary canal was accessed via a skin incision and a hole in the femoral condyle, and the contents of the medullary canal were disrupted and irrigated with saline solution. The implant was then introduced into the medullary canal, and the hole was sealed with bone wax. The incision was closed with sutures.

Sclerostin Antibody

Murine sclerostin antibody (Scl-Ab) (Amgen, Thousand Oaks, California) at 25 mg/kg was injected subcutaneously twice per week for the duration of the study. Control rats received saline solution injections. The dose was chosen on the basis of previous work in rat models[25,38,39,50].

Tissue Harvesting

Animals were killed by CO_2 inhalation and both femora were recovered. Femora to be studied by micro-CT and histology were fixed in 10% neutral buffered formalin, and femora to be studied by micro-CT and mechanical testing were wrapped in saline solution-soaked gauze and frozen (unfixed) at −20°C. The contralateral femora were fixed in 10% neutral buffered formalin. The harvested bones were imaged with contact radiography in cranial-caudal and lateral projections (MX-20; Faxitron X-Ray, Lincolnshire, Illinois) before the micro-CT was performed.

Micro-CT

The femora were scanned by micro-CT (μCT 40; Scanco, Wayne, Pennsylvania) with use of an isotropic voxel size of 16 μm (see Appendix). The trabecular

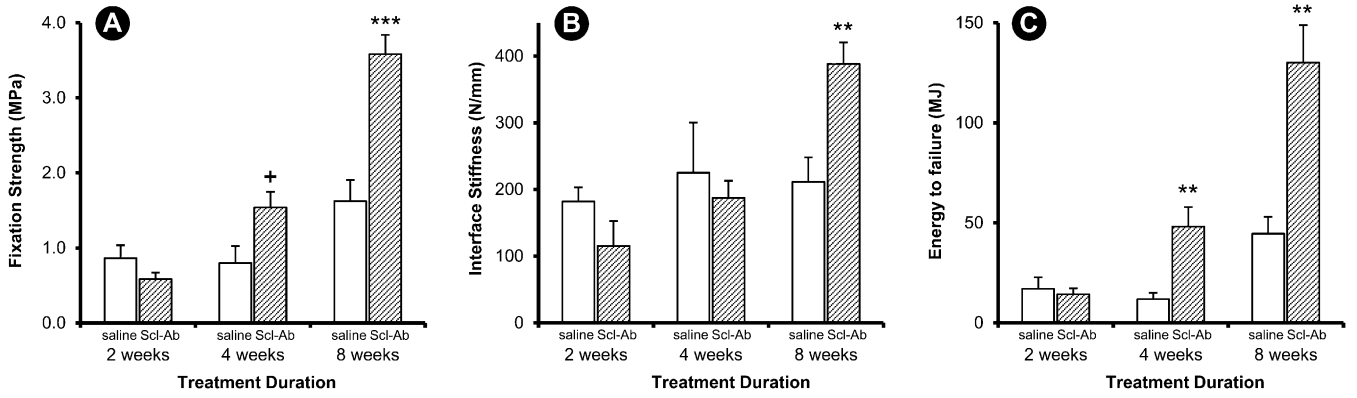

Fig. 1

Mechanical pull-out data. Implant fixation strength (**Fig. 1-A**), interface stiffness (**Fig. 1-B**), and energy to failure (**Fig. 1-C**) were determined in animals treated with saline solution (open bars) and Scl-Ab (shaded bars) at two, four, and eight weeks after implantation. Data are presented as the mean and the standard error of the mean; n = 11 for each two-week group and n = 12 for each four and eight-week group (*p < 0.05, **p < 0.01, and ***p < 0.001 for the treatment group compared with the control group, Bonferroni corrected. +p < 0.05, uncorrected).

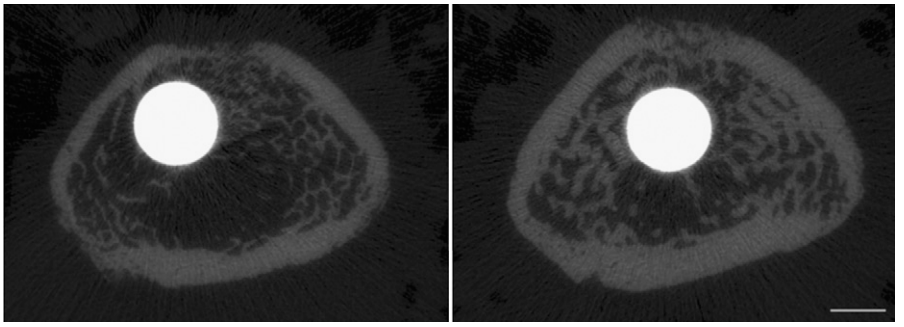

Fig. 2

Microcomputed tomography slices through the distal aspect of the implant at eight weeks (bar = 1 mm). The specimen from an animal treated with Scl-Ab (right) had noticeably thicker trabecular and cortical bone compared with the control treated with saline solution (left).

bone parameters that were determined included bone volume per total volume (BV/TV); trabecular number (Tb.N), thickness (Tb.Th), and spacing (Tb.Sp); and the structural model index (SMI). SMI characterizes the trabecular bone structure, with plate-like bone being assigned a lower value than rod-like bone. SMI can vary from slightly negative (plate-like) to approximately three (rod-like). The cortical bone parameters included total subperiosteal area (Tt.Ar), cortical bone area (Ct.Ar), medullary area (Ma.Ar), and cortical thickness (Ct.Th). This nomenclature and the determination of the corresponding values

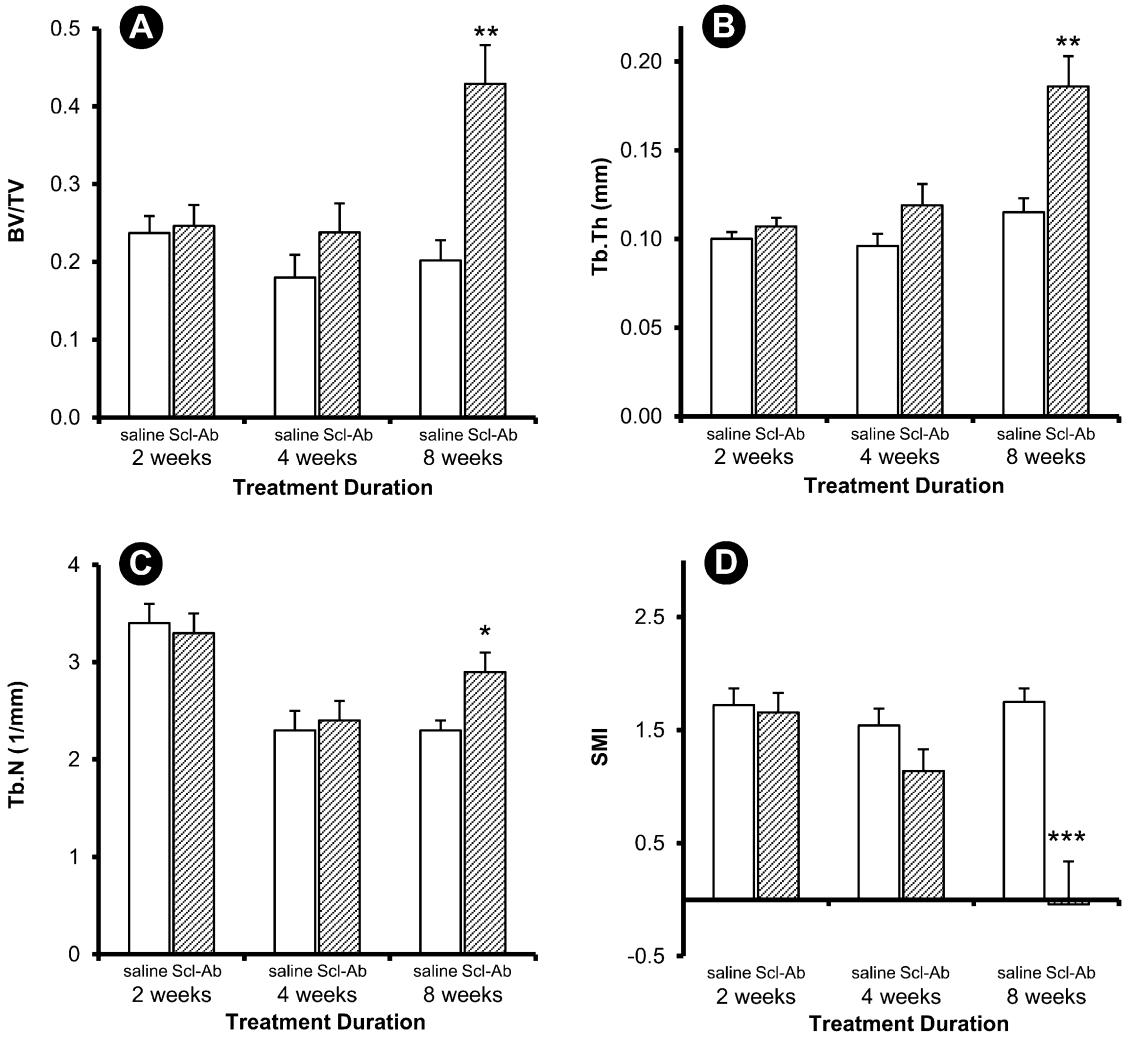

Fig. 3

Trabecular variables for the peri-implant site. Data are presented as the mean and the standard error of the mean; n = 15 for the four-week controls and n = 14 for all other groups (*$p < 0.05$ and ***$p < 0.001$ for the treatment group compared with the control group, Bonferroni corrected).

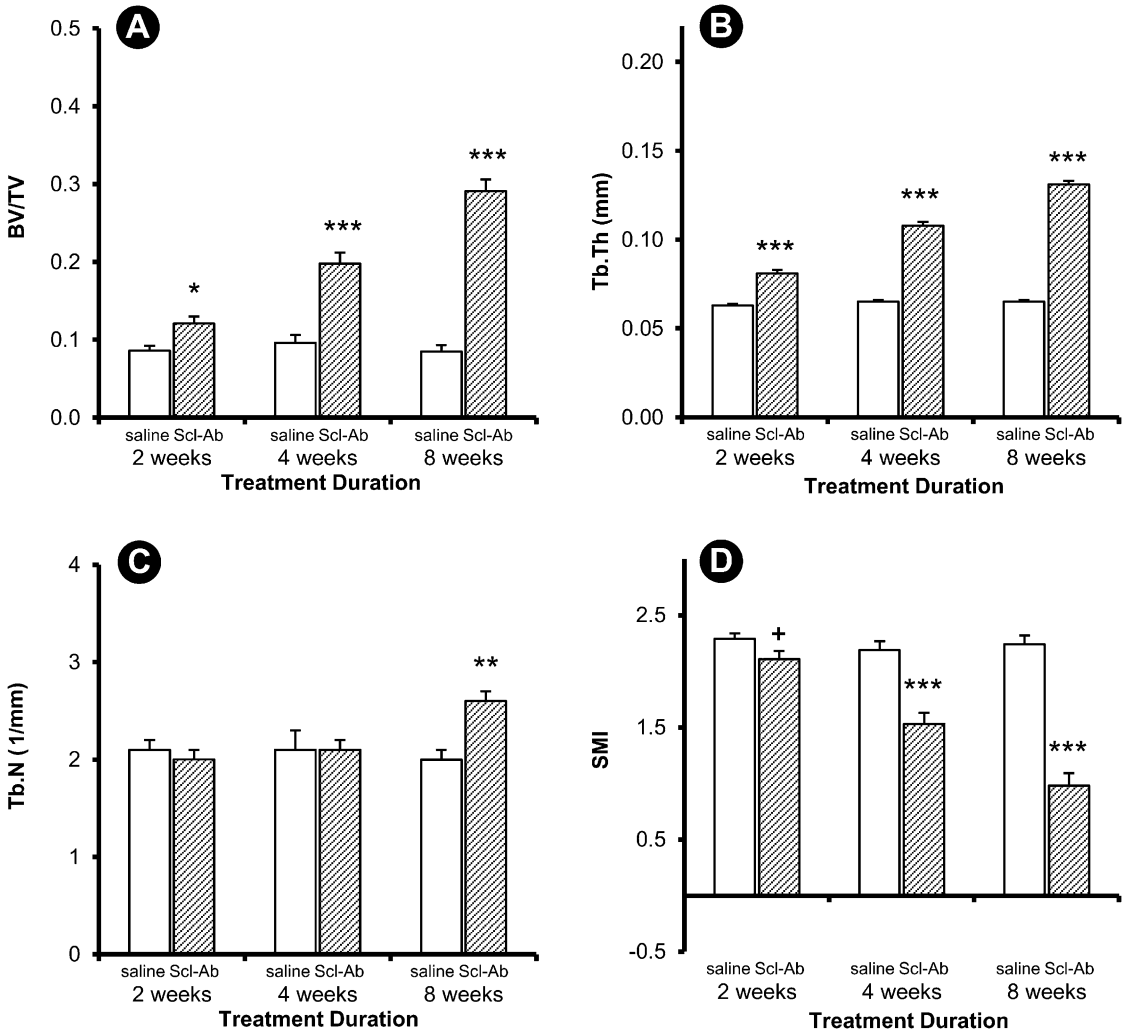

Fig. 4

Trabecular variables for the contralateral (intact) site. Data are presented as the mean and the standard error of the mean; n = 14 for each two-week group and n = 15 for all other groups (*$p < 0.05$, **$p < 0.01$, and ***$p < 0.001$ for the treatment group compared with the control group, Bonferroni corrected. +$p < 0.05$, uncorrected).

by micro-CT scanning followed a recently published guideline[51]. The regions of interest for the implanted femur and the contralateral femur were slightly different (see Appendix) and were not directly comparable.

Mechanical Testing

Pull-out tests were performed on thawed, fully hydrated, unfixed specimens[52]. The strength of fixation, interface stiffness, and energy to failure were calculated from the load-displacement curves.

Histology

Specimens were embedded in plastic, and a histological examination was performed according to established methods to qualitatively assess the nature of the tissue found within the medullary canal and at the bone-implant interface with use of conventional and polarized light microscopy[9,53-55].

Statistical Analyses

Parametric tests were used to assess differences between groups and included analyses of variance with both group and time as the between-subject factors. Means and standard errors of the mean are listed or shown graphically. Specific differences between the two groups at each time point were assessed with t tests only if there were significant between-subject effects or interactions. Exact p values are given. Pearson product-moment correlations and step-wise multiple regressions ($p_{in} = 0.05$, $p_{out} = 0.1$) were used to examine the relationship between mechanical parameters (dependent variables) and peri-implant bone architecture parameters (independent variables) (SPSS software, version 15.0; SPSS, Chicago, Illinois). Conventional statistical criteria for rejecting the null hypotheses were used (i.e., $p < 0.05$). For multiple post-hoc tests, the level of significance for the group effect was adjusted from the standard $p < 0.05$, 0.01, and 0.001 levels of significance to $p < 0.017$ (0.05/3), 0.0033, and 0.00033, according to the Bonferroni method, since one comparison was made at each of the three time periods.

Source of Funding

Funding for this study was provided by Amgen, Inc., U.S.A.; UCB S.A., Belgium; and the National Institutes of Health (NIH training grant T32 AR052272). The funding covered personnel, supplies, and indirect costs. Two of the authors are employees of Amgen, Inc.

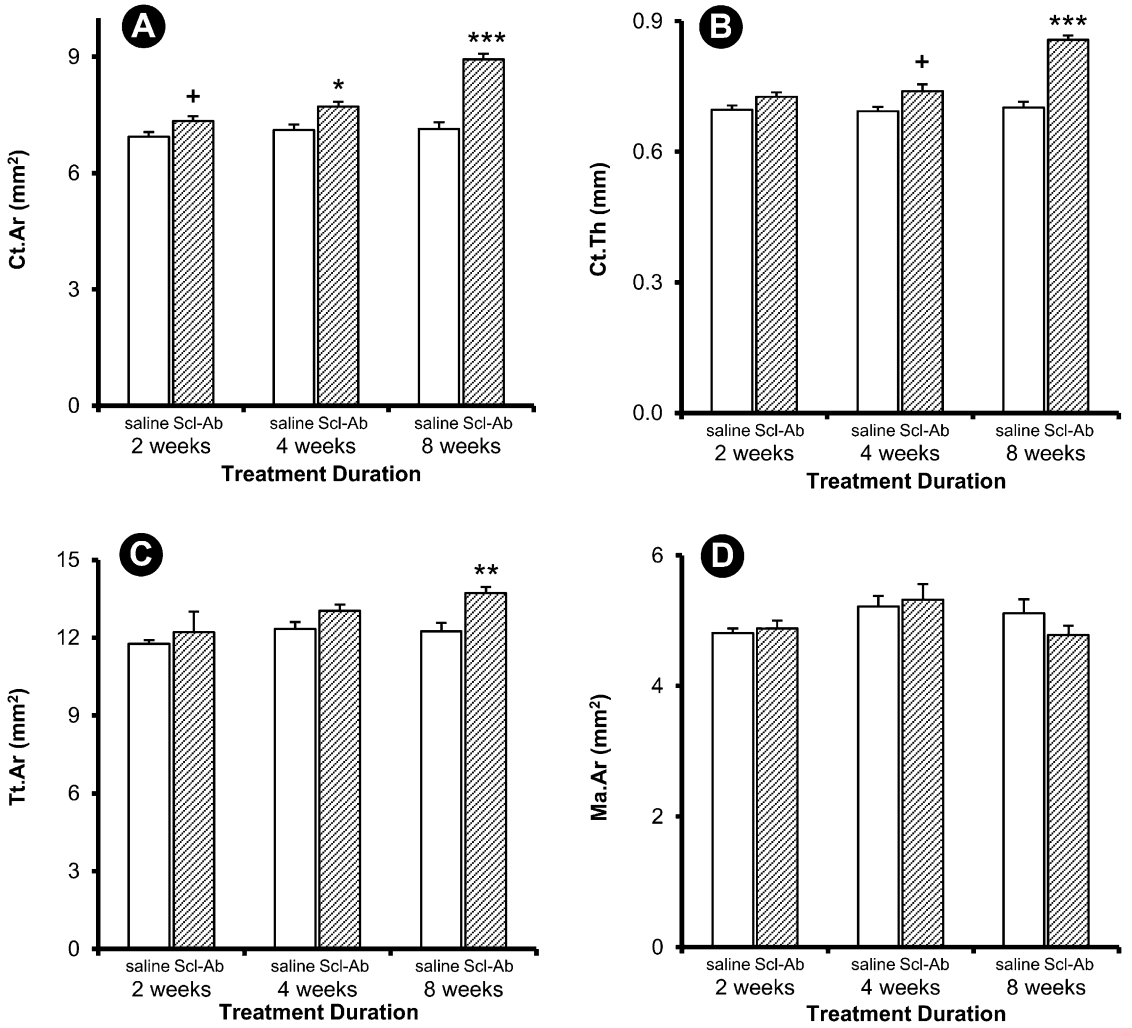

Fig. 5

Cortical variables for the peri-implant site. Data are presented as the mean and the standard error of the mean; n = 13 for the two-week control group, n = 15 for the four-week control group, and n = 14 for all other groups (*$p < 0.05$, **$p < 0.01$, and ***$p < 0.001$ for the treatment group compared with the control group, Bonferroni corrected. +$p < 0.05$, uncorrected).

Results

All but two of the animals tolerated the experimental procedures, exhibiting normal behaviors and gaining weight during the course of the study. Two animals, one in the two-week control group and one in the two-week Scl-Ab group, lost body weight and were excluded from the statistical analyses. Other animals were occasionally also excluded from a particular analysis because of technical errors; exact sample sizes are listed in the figures and tables. The average weight gain in the remaining eighty-eight animals was 20, 48, and 94 g at two, four, and eight weeks, respectively, with no difference between the control and treatment groups ($p = 0.154$ in the analysis of variance [ANOVA] for the group effect, $p < 0.001$ for the time effect, and $p = 0.885$ for the interaction between group and time). The animals were weight-bearing immediately after recovery from anesthesia and throughout the course of the study.

Implant fixation strength was significantly increased in the Scl-Ab treatment group compared with the control group (Fig. 1, $p < 0.001$ in the ANOVA), with significant time and group-by-time interaction effects as well ($p < 0.001$ for both terms in the ANOVA). Specifically, fixation strength was not different at two weeks, but it was 1.9-fold and 2.2-fold higher in the Scl-Ab group than in the control group at four and eight weeks, respectively (Fig. 1-A). The effect on interface stiffness was more subtle, as there was a significant group-by-time interaction term ($p = 0.010$) and a significant increase over time ($p = 0.003$) but no overall group effect ($p = 0.488$) because the treatment effect was only apparent at eight weeks (Fig. 1-B). Energy to failure had a similar pattern as fixation strength, with significant group, time, and group-by-time interaction terms ($p < 0.001$) and treatment-induced increases at four and eight weeks (Fig. 1-C).

Treatment-induced differences in peri-implant trabecular and cortical bone thickness were noticeable at eight weeks

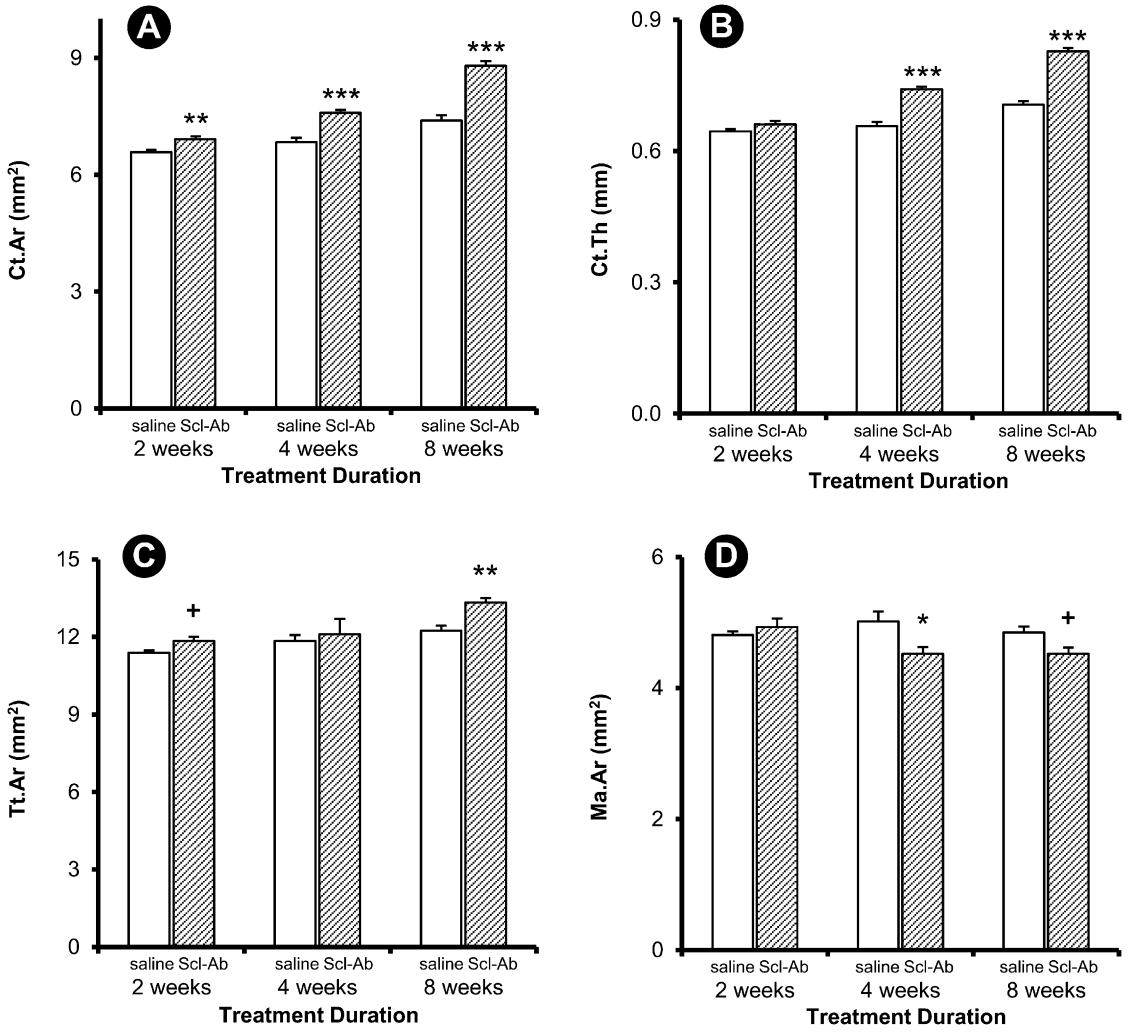

Fig. 6

Cortical variables for the contralateral (intact) site. Data are presented as the mean and the standard error of the mean; n = 14 for the two-week control group, n = 13 for the two-week treatment group, and n = 15 for all other groups (*$p < 0.05$, **$p < 0.01$, and ***$p < 0.001$ for the treatment group compared with the control group, Bonferroni corrected. +$p < 0.05$, uncorrected).

(Fig. 2). Quantitatively, differences in trabecular bone architecture between the control group and the group treated with Scl-Ab were evident in the implanted femur at eight weeks (Fig. 3), whereas differences in these variables were observed in the contralateral femur as early as two weeks (Fig. 4). Peri-implant trabecular BV/TV in the Scl-Ab treated rats was more than twice the value in the control group at eight weeks (Fig. 3-A). At eight weeks, Tb.Th and Tb.N were greater and SMI was smaller in the treated group compared with the control group (Figs. 3-B, 3-C, and 3-D). The differences in the trabecular bone in the contralateral (intact) femur (Fig. 4) were in the same direction as in the implanted femur (Fig. 3), but the treatment effect was apparent at all time points for all parameters except Tb.N at two and four weeks and SMI at two weeks.

Peri-implant Ct.Ar was significantly greater in the treated rats at four and eight weeks, whereas Ct.Th was greater only at eight weeks (Figs. 5-A and 5-B). Tt.Ar was greater at eight weeks, but there were no detectable differences in Ma.Ar (Figs. 5-C and 5-D). Similar treatment effects were observed in the contralateral femur, with greater Ct.Ar at all time points and greater Ct.Th at four and eight weeks (Figs. 6-A and 6-B). Tt.Ar was greater at eight weeks, and Ma.Ar was smaller at four weeks (Figs. 6-C and 6-D).

Histologically, new woven bone was observed in the vicinity of the implant at two weeks in most specimens. This was particularly apparent adjacent to the proximal one-half of the implant where this new bone occupied the space between the endocortical surface and the implant, a region of the medullary canal that is normally devoid of bone in intact femora. The amount of this new bone was variable, but on the basis of inspection it was not consistently greater in the animals treated with Scl-Ab. Adjacent to the distal one-half of the implant (i.e., the part of the implant that was mostly in metaphyseal trabecular bone), new bone formed on preexisting trabeculae. This new bone was largely woven at the two-week time point,

TABLE I Univariate Correlations Between Trabecular Bone Architectural Properties and Implant Fixation Properties

		Independent Variable				
Dependent Variable	Group*	Bone Volume/ Total Volume (BV/TV)	Structural Model Index (SMI)	Trabecular Thickness (Tb.Th)	Trabecular Spacing (Tb.Sp)	Trabecular Number (Tb.N)
Fixation strength						
	Saline solution	−0.016	−0.187	0.019	0.124	−0.148
	Scl-Ab	0.596†	−0.678†	0.719†	0.078	−0.121
Stiffness						
	Saline solution	0.115	−0.540‡	0.017	0.062	−0.031
	Scl-Ab	0.436§	−0.519‡	0.517‡	0.053	−0.120
Energy						
	Saline solution	−0.015	−0.027	0.082	0.065	−0.129
	Scl-Ab	0.577†	−0.662†	0.717†	0.069	−0.094

*Scl-Ab = sclerostin antibody. †$P < 0.001$. ‡$P < 0.01$. §$P < 0.05$.

whereas at later time points the new bone was lamellar in appearance. By eight weeks, the trabeculae in the animals treated with Scl-Ab appeared to be thicker than those in the control animals. Bone-implant contact was variable, and it was not quantified as only three samples per time point per group were available for histological examination. However, the rim of bone in contact with the implant appeared to be thicker at the later time points, particularly in the animals treated with Scl-Ab. There appeared to have been more new lamellar bone formation along the endocortical surface in the antibody-treated animals compared with the control animals, particularly at four and eight weeks after Scl-Ab treatment (Fig. 7). In the quantitative assessment, however, there were no corresponding differences in Ma.Ar (Fig. 5-D).

Implant fixation strength had significant univariate correlations with some peri-implant trabecular variables (BV/TV,

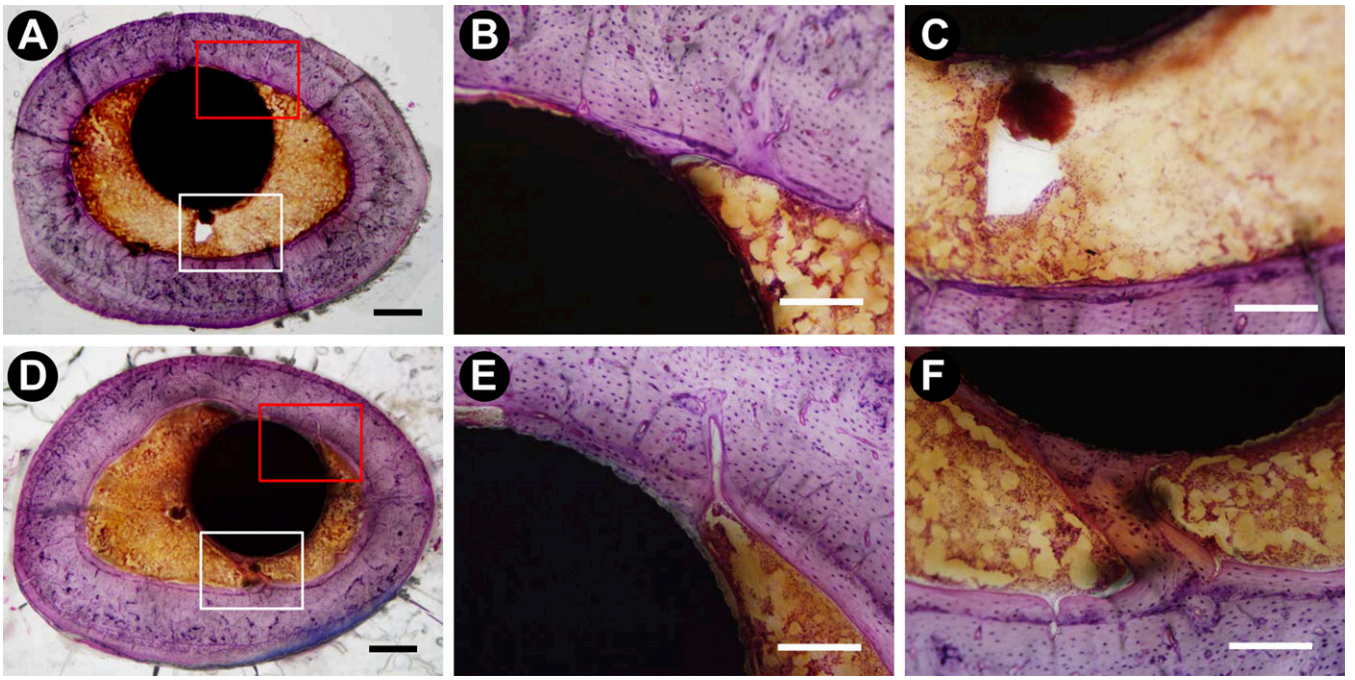

Fig. 7

Histological observation of regenerating bone around the implant after saline solution treatment (**Figs. 7-A, 7-B, and 7-C**) and Scl-Ab treatment (**Figs. 7-D, 7-E, and 7-F**) for eight weeks (bar = 500 μm for panels A and D and 200 μm for panels B, C, E, and F; plastic-embedded samples stained with basic fuchsin and toluidine blue).

TABLE II Univariate Correlations Between Cortical Bone Geometry and Implant Fixation Properties

		Independent Variable			
Dependent Variable	Group*	Cortical Area (Ct.Ar)	Cortical Thickness (Ct.Th)	Total Area (Tt.Ar)	Medullary Area (Ma.Ar)
Fixation strength					
	Saline solution	0.052	0.111	−0.193	−0.260
	Scl-Ab	0.671†	0.666†	0.502‡	−0.255
Stiffness					
	Saline solution	−0.222	−0.094	−0.266	−0.255
	Scl-Ab	0.428§	0.485‡	0.205	−0.358§
Energy					
	Saline solution	0.047	0.180	−0.102	−0.204
	Scl-Ab	0.636†	0.595†	0.538‡	−0.135

*Scl-Ab = sclerostin antibody. †$P < 0.001$. ‡$P < 0.01$. §$P < 0.05$.

SMI, and Tb.Th) (Table I) and some cortical variables (Ct.Ar, Ct.Th, and Tt.Ar) (Table II). The strongest univariate correlations for fixation strength were with Tb.Th ($r = 0.719$, $p < 0.001$), SMI ($r = -0.678$, $p < 0.001$), and Ct.Ar ($r = 0.671$, $p < 0.001$) in the Scl-Ab treatment group. Only one of the correlations was significant in the saline-solution control group (Table I). In general, the correlations of implant fixation strength and energy with the bone variables followed similar patterns, whereas the correlations between the peri-implant bone variables and interface stiffness were less pronounced.

Step-wise multiple regressions showed that the peri-implant bone variables explained 61% of the variance in fixation strength, 32% of the variance in stiffness, and 63% of the variance in energy to failure ($p < 0.001$ for each model). Both trabecular and cortical variables were significant predictors of fixation strength (Tb.Th, Ct.Th, Tb.N, and SMI), stiffness (SMI, Tb.N, and Ma.Ar), and energy to failure (Tb.Th, Ct.Th, and Tb.N).

Discussion

In this study, systemic delivery of sclerostin antibody led to increased mechanical fixation of an intramedullary implant and increased trabecular and cortical bone volume in the peri-implant region. The values for fixation strength and energy to failure at four weeks in the Scl-Ab group were approximately equivalent to the eight-week values in the control group, suggesting that treatment accelerated the healing response. Although trabecular and cortical end points changed in the contralateral bone as early as two weeks, differences in all peri-implant bone measurements with the exception of cortical area were not apparent until eight weeks. Changes in the peri-implant cortical area were first apparent by two weeks. Finally, approximately 60% of the variance in fixation strength and in energy to failure were ascribed to peri-implant trabecular and cortical bone properties. Accordingly, we suggest that Scl-Ab treatment may hold promise for improving implant fixation in total joint replacement.

The implant model used in this study is an adaptation of the bone marrow ablation model originally used to examine hematopoiesis[56,57] and subsequently used to study intramembranous bone formation[49,58-61]. Collectively, these studies have shown that an inflammatory phase typical of wound-healing and characterized by clot formation is followed by a repair phase that occurs within approximately two weeks of injury. A subsequent bone remodeling phase then occurs; during this time, resorption exceeds formation and the newly formed bone in the part of the medullary canal that is normally devoid of bone is removed, with restoration of the normal marrow contents by approximately four weeks[62]. In the present study, because the effect of the antibody treatment on implant fixation was not apparent until four weeks, we suggest that the mechanism of action was on the formation of lamellar as opposed to woven bone. The data from the contralateral femur, in which there was no induced injury, showed increased trabecular bone volume, thickness, and apparent density as well as increased cortical area by two weeks; this indicates a rapid response to sclerostin antibody treatment, consistent with previous observations[25]. If one assumes that the bone-forming potential was already elevated during the repair phase, then it is perhaps not surprising that the sclerostin antibody treatment, which is known to stimulate lamellar bone formation, had its most dramatic effect during the remodeling phase of the model (four and eight weeks).

The mechanical stability of the implant, as assessed by fixation strength, stiffness, and energy, was related to both peri-implant trabecular architecture and cortical bone geometry. In general, architectural variables such as trabecular thickness, cortical thickness, the structural model index, and trabecular number were the most important variables for predicting the mechanical end points, presumably because in this medullary implantation model the implant is in close contact with cortical bone proximally and with trabecular bone distally. In addition, these analyses suggest that the thickness and number of trabeculae in the vicinity of the implant may be critically

important in providing mechanical stability; this is consistent with the findings reported in a recent study[63]. For cortical bone, cortical thickness and medullary area were consistently included in the regression models, presumably because of the addition of bone at the endocortical surface. Other authors have reported that sclerostin antibody increases bone formation at this surface[50].

Enhancing implant fixation through the use of anabolic agents has been studied in the context of locally delivered growth factors such as BMP and transforming growth factor-beta[7]. More recently, several anabolic drugs or agents have been developed for treatment of osteoporosis[26,64]. These systemically delivered treatments include intermittent parathyroid hormone (PTH) therapy, which enhanced implant fixation in several rat models[14,65-69]. In general, these studies have shown that PTH increased implant fixation strength by a factor of two to three, depending on the model used, with the earliest effects observed at two weeks. There is a potential for positive interaction between the molecular mechanisms by which bone formation is stimulated by PTH and Scl-Ab through the LRP5/6/Wnt pathway[70,71], and this merits additional attention.

Most recently, it has been reported that administration of sclerostin antibody increased the pull-out strength after two or four weeks of treatment in a metaphyseal healing model in which a steel screw was inserted into the tibial metaphyseal region of rats[39]. The model used in the tibial screw study was different from that in the current study in many aspects, such as the anatomical location (trabecular-rich metaphyseal bone compared with the medullary canal), the size and shape of the implant (a screw fitted in the proximal aspect of the tibia compared with a rod occupying a large portion of the femoral medullary canal), and the implant material (stainless steel compared with titanium). Together, these studies show that Scl-Ab was efficacious in increasing bone formation and enhancing implant fixation in both the metaphyseal region as well as the medullary canal.

If one defines the initial healing phase to include the first two months of the response to placement of the implant, then the present study indicates that Scl-Ab treatment clearly accelerated progression through this phase. In addition, the treatment led to an increase in bone volume adjacent to the implant that far exceeded the amount that would have been expected in the control group even if longer-term data had been included. On the basis of the present study, it is not possible to know whether an initial short duration of sclerostin antibody treatment would positively contribute to the steady-state or long-term interface fixation. We would expect the bone formed during the treatment period to respond normally to the long-term mechanical environment. However, the presence of high bone mass adjacent to the implant could influence later remodeling by altering how mechanical forces are transferred from the implant to the host bone. Following this logic, the newly formed bone might be expected to alter the mechanical environment and therefore have a secondary effect on long-term remodeling. In addition, the presence of more bone adjacent to the implant might help prevent ingress of wear debris and subsequent bone resorption at the interface[8]. However, in the absence of longer-term weight-bearing studies, it is unknown whether or not these possible longer-term benefits of Scl-Ab treatment would be realized.

Sclerostin is thought to be secreted exclusively by osteocytes in the adult skeleton[72], and it is therefore an attractive therapeutic target because it is likely that there will be few nonskeletal effects of treatment. Although giving a systemic agent for a local need (in this case, implant fixation) means that the entire skeleton is being treated for a local desired effect, in the short term this strategy would appear to pose few risks. However, given the strong response of the skeleton to this anabolic agent[25,26], it appears likely that eventual clinical use will include drug holidays since prolonged, continuous use could lead to excessive bone volume. For bone-healing applications, it might be desirable to have a means of delivering the treatment locally.

In conclusion, the present study indicates that changes in bone volume and architecture in the peri-implant region following systemic treatment with Scl-Ab were associated with increased mechanical fixation of implants in a rat model.

Appendix

eA A figure showing the regions of interest in the micro-CT analysis and a detailed description of the methods are available with the online version of this article as a data supplement at jbjs.org. ■

Amarjit S. Virdi, PhD
Kotaro Sena, DDS, PhD
James Maletich, BS
Margaret McNulty, PhD
Dale R. Sumner, PhD
Department of Anatomy and Cell Biology,
Rush Medical College, Rush University Medical Center,
600 South Paulina Street, Room 507, AcFac,
Chicago, IL 60612.
E-mail address for D.R. Sumner: rick_sumner@rush.edu

Min Liu, PhD
Hua Zhu Ke, MD
Metabolic Disorders Research, Mail Stop 29-M-B, Amgen,
One Amgen Center Drive, Thousand Oaks, CA 91320

References

1. Bozic KJ, Kurtz SM, Lau E, Ong K, Vail TP, Berry DJ. The epidemiology of revision total hip arthroplasty in the United States. J Bone Joint Surg Am. 2009;91:128-33.

2. Kurtz S, Mowat F, Ong K, Chan N, Lau E, Halpern M. Prevalence of primary and revision total hip and knee arthroplasty in the United States from 1990 through 2002. J Bone Joint Surg Am. 2005;87:1487-97.

3. Kurtz S, Ong K, Lau E, Mowat F, Halpern M. Projections of primary and revision hip and knee arthroplasty in the United States from 2005 to 2030. J Bone Joint Surg Am. 2007;89:780-5.

4. Hungerford DS, Mont MA. Revision of the femoral component: proximal porous coating. In: Callaghan JJ, Rosenberg AG, Rubash HE. The adult hip. Philadelphia: Lippincott-Raven; 1998. p 1503-13.

5. Callaghan JJ, Johnston RC. Revision of the femoral component: cement. In: Callaghan JJ, Rosenberg AG, Rubash HE. The adult hip. Philadelphia: Lippincott-Raven; 1998. p 1515-26.

6. Mavrogenis AF, Dimitriou R, Parvizi J, Babis GC. Biology of implant osseointegration. J Musculoskelet Neuronal Interact. 2009;9:61-71.

7. Sumner DR, Virdi AS. Bioactive coatings for implant fixation. In: Berry DJ, Lieberman JR, editors. Surgery of the hip. New York, Elsevier, 2010.

8. Bobyn JD, Jacobs JJ, Tanzer M, Urban RM, Aribindi R, Sumner DR, Turner TM, Brooks CE. The susceptibility of smooth implant surfaces to periimplant fibrosis and migration of polyethylene wear debris. Clin Orthop Relat Res. 1995;311:21-39.

9. Sumner DR, Turner TM, Urban RM, Turek T, Seeherman H, Wozney JM. Locally delivered rhBMP-2 enhances bone ingrowth and gap healing in a canine model. J Orthop Res. 2004;22:58-65.

10. Aspenberg P, Jeppsson C, Wang JS, Boström M. Transforming growth factor beta and bone morphogenetic protein 2 for bone ingrowth: a comparison using bone chambers in rats. Bone. 1996;19:499-503.

11. Cochran DL, Schenk R, Buser D, Wozney JM, Jones AA. Recombinant human bone morphogenetic protein-2 stimulation of bone formation around endosseous dental implants. J Periodontol. 1999;70:139-50.

12. Bragdon CR, Doherty AM, Rubash HE, Jasty M, Li XJ, Seeherman H, Harris WH. The efficacy of BMP-2 to induce bone ingrowth in a total hip replacement model. Clin Orthop Relat Res. 2003;417:50-61.

13. Sigurdsson TJ, Fu E, Tatakis DN, Rohrer MD, Wikesjö UM. Bone morphogenetic protein-2 for peri-implant bone regeneration and osseointegration. Clin Oral Implants Res. 1997;8:367-74.

14. Skripitz R, Aspenberg P. Implant fixation enhanced by intermittent treatment with parathyroid hormone. J Bone Joint Surg Br. 2001;83:437-40.

15. van Bezooijen RL, Roelen BA, Visser A, van der Wee-Pals L, de Wilt E, Karperien M, Hamersma H, Papapoulos SE, ten Dijke P, Löwik CW. Sclerostin is an osteocyte-expressed negative regulator of bone formation, but not a classical BMP antagonist. J Exp Med. 2004;199:805-14.

16. Winkler DG, Sutherland MK, Geoghegan JC, Yu C, Hayes T, Skonier JE, Shpektor D, Jonas M, Kovacevich BR, Staehling-Hampton K, Appleby M, Brunkow ME, Latham JA. Osteocyte control of bone formation via sclerostin, a novel BMP antagonist. EMBO J. 2003;22:6267-76.

17. Poole KE, van Bezooijen RL, Loveridge N, Hamersma H, Papapoulos SE, Löwik CW, Reeve J. Sclerostin is a delayed secreted product of osteocytes that inhibits bone formation. FASEB J. 2005;19:1842-4. Epub 2005 Aug 25.

18. Paszty C, Turner CH, Robinson MK. Sclerostin: a gem from the genome leads to bone-building antibodies. J Bone Miner Res. 2010;25:1897-904.

19. Balemans W, Cleiren E, Siebers U, Horst J, Van Hul W. A generalized skeletal hyperostosis in two siblings caused by a novel mutation in the SOST gene. Bone. 2005;36:943-7.

20. Li X, Ominsky MS, Niu QT, Sun N, Daugherty B, D'Agostin D, Kurahara C, Gao Y, Cao J, Gong J, Asuncion F, Barrero M, Warmington K, Dwyer D, Stolina M, Morony S, Sarosi I, Kostenuik PJ, Lacey DL, Simonet WS, Ke HZ, Paszty C. Targeted deletion of the sclerostin gene in mice results in increased bone formation and bone strength. J Bone Miner Res. 2008;23:860-9.

21. Lin C, Jiang X, Dai Z, Guo X, Weng T, Wang J, Li Y, Feng G, Gao X, He L. Sclerostin mediates bone response to mechanical unloading through antagonizing Wnt/beta-catenin signaling. J Bone Miner Res. 2009;24:1651-61.

22. Li X, Zhang Y, Kang H, Liu W, Liu P, Zhang J, Harris SE, Wu D. Sclerostin binds to LRP5/6 and antagonizes canonical Wnt signaling. J Biol Chem. 2005;280:19883-7. Epub 2005 Mar 18.

23. Johnson ML, Harnish K, Nusse R, Van Hul W. LRP5 and Wnt signaling: a union made for bone. J Bone Miner Res. 2004;19:1749-57. Epub 2004 Aug 23.

24. Ott SM. Sclerostin and Wnt signaling—the pathway to bone strength. J Clin Endocrinol Metab. 2005;90:6741-3.

25. Li X, Ominsky MS, Warmington KS, Morony S, Gong J, Cao J, Gao Y, Shalhoub V, Tipton B, Haldankar R, Chen Q, Winters A, Boone T, Geng Z, Niu QT, Ke HZ, Kostenuik PJ, Simonet WS, Lacey DL, Paszty C. Sclerostin antibody treatment increases bone formation, bone mass, and bone strength in a rat model of postmenopausal osteoporosis. J Bone Miner Res. 2009;24:578-88.

26. Padhi D, Jang G, Stouch B, Fang L, Posvar E. Single-dose, placebo-controlled, randomized study of AMG 785, a sclerostin monoclonal antibody. J Bone Miner Res. 2011;26:19-26.

27. Sandberg MM, Aro HT, Vuorio EI. Gene expression during bone repair. Clin Orthop Relat Res. 1993;289:292-312.

28. 'Nakase T, Nomura S, Yoshikawa H, Hashimoto J, Hirota S, Kitamura Y, Oikawa S, Ono K, Takaoka K. Transient and localized expression of bone morphogenetic protein 4 messenger RNA during fracture healing. J Bone Miner Res. 1994;9:651-9.

29. Bostrom MP, Lane JM, Berberian WS, Missri AA, Tomin E, Weiland A, Doty SB, Glaser D, Rosen VM. Immunolocalization and expression of bone morphogenetic proteins 2 and 4 in fracture healing. J Orthop Res. 1995;13:357-67.

30. Yoshimura Y, Nomura S, Kawasaki S, Tsutsumimoto T, Shimizu T, Takaoka K. Colocalization of noggin and bone morphogenetic protein-4 during fracture healing. J Bone Miner Res. 2001;16:876-84.

31. Yu Y, Yang JL, Chapman-Sheath PJ, Walsh WR. TGF-beta, BMPS, and their signal transducing mediators, Smads, in rat fracture healing. J Biomed Mater Res. 2002;60:392-7.

32. Campisi P, Hamdy RC, Lauzier D, Amako M, Rauch F, Lessard ML. Expression of bone morphogenetic proteins during mandibular distraction osteogenesis. Plast Reconstr Surg. 2003;111:201-8; discussion 209-10.

33. Kloen P, Di Paola M, Borens O, Richmond J, Perino G, Helfet DL, Goumans MJ. BMP signaling components are expressed in human fracture callus. Bone. 2003;33:362-71.

34. Niikura T, Hak DJ, Reddi AH. Global gene profiling reveals a downregulation of BMP gene expression in experimental atrophic nonunions compared to standard healing fractures. J Orthop Res. 2006;24:1463-71.

35. Zhong N, Gersch RP, Hadjiargyrou M. Wnt signaling activation during bone regeneration and the role of Dishevelled in chondrocyte proliferation and differentiation. Bone. 2006;39:5-16. Epub 2006 Feb 3.

36. Issack PS, Helfet DL, Lane JM. Role of Wnt signaling in bone remodeling and repair. HSS J. 2008;4:66-70. Epub 2007 Dec 8.

37. Chen Y, Alman BA. Wnt pathway, an essential role in bone regeneration. J Cell Biochem. 2009;106:353-62.

38. Ominsky MS, Li C, Li X, Tan HL, Lee E, Barrero M, Asuncion FJ, Dwyer D, Han CY, Vlasseros F, Samadfam R, Jolette J, Smith SY, Stolina M, Lacey DL, Simonet WS, Paszty C, Li G, Ke HZ. Inhibition of sclerostin by monoclonal antibody enhances bone healing and improves bone density and strength of non-fractured bones. J Bone Miner Res. 2010. 2010;26:1012-21.

39. Agholme F, Li X, Isaksson H, Ke HZ, Aspenberg P. Sclerostin antibody treatment enhances metaphyseal bone healing in rats. J Bone Miner Res. 2010;25:2412-8.

40. De Ranieri A, Virdi AS, Kuroda S, Shott S, Dai Y, Sumner DR. Local application of rhTGF-beta2 modulates dynamic gene expression in a rat implant model. Bone. 2005;36:931-40. Epub 2005 Mar 24.

41. De Ranieri A, Virdi AS, Kuroda S, Shott S, Leven RM, Hallab NJ, Sumner DR. Local application of rhTGF-beta2 enhances peri-implant bone volume and bone-implant contact in a rat model. Bone. 2005;37:55-62.

42. De Ranieri A, Virdi AS, Kuroda S, Healy KE, Hallab NJ, Sumner DR. Saline irrigation does not affect bone formation or fixation strength of hydroxyapatite/tricalcium phosphate-coated implants in a rat model. J Biomed Mater Res B Appl Biomater. 2005;74:712-7.

43. Kuroda S, Virdi AS, Li P, Healy KE, Sumner DR. A low-temperature biomimetic calcium phosphate surface enhances early implant fixation in a rat model. J Biomed Mater Res A. 2004;70:66-73.

44. Ishizaka M, Tanizawa T, Sofue M, Dohmae Y, Endo N, Takahashi HE. Bone particles disturb new bone formation on the interface of the titanium implant after reaming of the marrow cavity. Bone. 1996;19:589-94.

45. Hara T, Hayashi K, Nakashima Y, Kanemaru T, Iwamoto Y. The effect of hydroxyapatite coating on the bonding of bone to titanium implants in the femora of ovariectomised rats. J Bone Joint Surg Br. 1999;81:705-9.

46. Schmidmaier G, Wildemann B, Schwabe P, Stange R, Hoffmann J, Südkamp NP, Haas NP, Raschke M. A new electrochemically graded hydroxyapatite coating for osteosynthetic implants promotes implant osteointegration in a rat model. J Biomed Mater Res. 2002;63:168-72.

47. Dupont WD, Plummer WD Jr. Power and sample size calculations. A review and computer program. Control Clin Trials. 1990;11:116-28.

48. Ho JE, Barber TA, Virdi AS, Sumner DR, Healy KE. The effect of enzymatically degradable IPN coatings on peri-implant bone formation and implant fixation. J Biomed Mater Res A. 2007;81:720-7.

49. Suva LJ, Seedor JG, Endo N, Quartuccio HA, Thompson DD, Bab I, Rodan GA. Pattern of gene expression following rat tibial marrow ablation. J Bone Miner Res. 1993;8:379-88.

50. Li X, Warmington KS, Niu QT, Asuncion FJ, Barrero M, Grisanti M, Dwyer D, Stouch B, Thway TM, Stolina M, Ominsky MS, Kostenuik PJ, Simonet WS, Paszty C, Ke HZ. Inhibition of sclerostin by monoclonal antibody increases bone formation, bone mass, and bone strength in aged male rats. J Bone Miner Res. 2010;25:2647-56. doi: 10.1002/jbmr.182. Epub 2010 Jul 16.

51. Bouxsein ML, Boyd SK, Christiansen BA, Guldberg RE, Jepsen KJ, Müller R. Guidelines for assessment of bone microstructure in rodents using micro-computed tomography. J Bone Miner Res. 2010;25:1468-86.

52. Berzins A, Sumner DR. Implant pushout and pullout tests. In: An YH, Draughn RA. Mechanical testing of bone and the bone-implant interface. Boca Raton: CRC Press; 2000. p 463-76.

53. Sumner DR, Turner TM, Purchio AF, Gombotz WR, Urban RM, Galante JO. Enhancement of bone ingrowth by transforming growth factor-beta. J Bone Joint Surg Am. 1995;77:1135-47.

54. Sumner DR, Turner TM, Urban RM, Leven RM, Hawkins M, Nichols EH, McPherson JM, Galante JO. Locally delivered rhTGF-beta2 enhances bone ingrowth and bone regeneration at local and remote sites of skeletal injury. J Orthop Res. 2001;19:85-94.

55. Sumner DR, Turner TM, Cohen M, Losavio P, Urban RM, Nichols EH, McPherson JM. Aging does not lessen the effectiveness of TGFbeta2-enhanced bone regeneration. J Bone Miner Res. 2003;18:730-6.

56. Amsel S, Maniatis A, Tavassoli M, Crosby WH. The significance of intramedullary cancellous bone formation in the repair of bone marrow tissue. Anat Rec. 1969;164:101-11.

57. Patt HM, Maloney MA. Bone marrow regeneration after local injury: a review. Exp Hematol. 1975;3:135-48.

58. Bab IA. Postablation bone marrow regeneration: an in vivo model to study differential regulation of bone formation and resorption. Bone. 1995;17(4 Suppl): 437S-441S.

59. Gazit D, Zilberman Y, Turgeman G, Zhou S, Kahn A. Recombinant TGF-beta1 stimulates bone marrow osteoprogenitor cell activity and bone matrix synthesis in osteopenic, old male mice. J Cell Biochem. 1999;73:379-89.

60. Liang CT, Barnes J, Seedor JG, Quartuccio HA, Bolander M, Jeffrey JJ, Rodan GA. Impaired bone activity in aged rats: alterations at the cellular and molecular levels. Bone. 1992;13:435-41.

61. Tanaka H, Barnes J, Liang CT. Effect of age on the expression of insulin-like growth factor-I, interleukin-6, and transforming growth factor-beta mRNAs in rat femurs following marrow ablation. Bone. 1996;18:473-8.

62. Wise JK, Sena K, Vranizan K, Pollock JF, Healy KE, Hughes WF, Sumner DR, Virdi AS. Temporal gene expression profiling during rat femoral marrow ablation-induced intramembranous bone regeneration. PLoS One. 2010;5. pii: e12987.

63. Gabet Y, Kohavi D, Voide R, Mueller TL, Müller R, Bab I. Endosseous implant anchorage is critically dependent on mechanostructural determinants of peri-implant bone trabeculae. J Bone Miner Res. 2010;25:575-83.

64. Shoback D. Update in osteoporosis and metabolic bone disorders. J Clin Endocrinol Metab. 2007;92:747-53.

65. Dayer R, Badoud I, Rizzoli R, Ammann P. Defective implant osseointegration under protein undernutrition: prevention by PTH or pamidronate. J Bone Miner Res. 2007;22:1526-33.

66. Skripitz R, Aspenberg P. Early effect of parathyroid hormone (1-34) on implant fixation. Clin Orthop Relat Res. 2001;392:427-32.

67. Skripitz R, Böhling S, Rüther W, Aspenberg P. Stimulation of implant fixation by parathyroid hormone (1-34)-A histomorphometric comparison of PMMA cement and stainless steel. J Orthop Res. 2005;23:1266-70. Epub 2005 Jun 16.

68. Skripitz R, Johansson HR, Ulrich SD, Werner A, Aspenberg P. Effect of alendronate and intermittent parathyroid hormone on implant fixation in ovariectomized rats. J Orthop Sci. 2009;14:138-43. Epub 2009 Apr 1.

69. Dayer R, Brennan TC, Rizzoli R, Ammann P. PTH improves titanium implant fixation more than pamidronate or renutrition in osteopenic rats chronically fed a low protein diet. Osteoporos Int. 2010;21:957-67. Epub 2009 Oct 27.

70. Bellido T. Downregulation of SOST/sclerostin by PTH: a novel mechanism of hormonal control of bone formation mediated by osteocytes. J Musculoskelet Neuronal Interact. 2006;6:358-9.

71. O'Brien CA, Plotkin LI, Galli C, Goellner JJ, Gortazar AR, Allen MR, Robling AG, Bouxsein M, Schipani E, Turner CH, Jilka RL, Weinstein RS, Manolagas SC, Bellido T. Control of bone mass and remodeling by PTH receptor signaling in osteocytes. PLoS One. 2008;3:e2942.

72. Balemans W, Ebeling M, Patel N, Van Hul E, Olson P, Dioszegi M, Lacza C, Wuyts W, Van Den Ende J, Willems P, Paes-Alves AF, Hill S, Bueno M, Ramos FJ, Tacconi P, Dikkers FG, Stratakis C, Lindpaintner K, Vickery B, Foernzler D, Van Hul W. Increased bone density in sclerosteosis is due to the deficiency of a novel secreted protein (SOST). Hum Mol Genet. 2001;10:537-43.